Applied Chemical Engineering (2025) Volume 8 Issue 4 ISSN: 2578-2010 (O)
doi: 10.59429/ace.v8i4.5796

ORIGINAL RESEARCH ARTICLE

A comparative study of the theoretical and practical values of ionization constants for amino acid derivatives in the neutral and anionic states

Mohammed Abdulrazaq Mahdy[1], Noor H. M. Saeed[2,*]

[1] *General Directorate of Education in Nineveh, Mosul, 42001, Iraq*

[2] *Chemistry Department, College of Education for pure sciences, University of Mosul, Mosul, 42001, Iraq*

***Corresponding author:** Noor H. M. Saeed, noorsaeed@uomosul.edu.iq

ABSTRACT

A theoretical study was conducted to determine the ionization constants of several amino acid derivatives (2,4-dinitrophenyl amino acids) through density functional theory and using two types of basic bases, CC PV-DZ and (6311-G)d,p. The accuracy of these two bases was determined in the negative and neutral states of the studied compounds. This was achieved by studying several physical variables and theoretically calculated energy functions, and the extent of their correlation with the values of the ionization constants calculated practically, where these variables were linked to the known values of amino acids. The results derived from this correlation were found to be good. The basic rule showed greater accuracy in the theoretical results when compared to the experimental results. There was also greater agreement between the results for the compounds in the negative state, more recently than in the neutral state, due to the electronic interpretations of the chemical structures of the compounds studied in the negative state.

Keywords: density functional theory; ionization constants; theoretically calculation; basisi set; amino acids derivative

ARTICLE INFO

Received: 11 October2025
Accepted: 7 November 2025
Available online: 24 November 2025

COPYRIGHT

Copyright © 2025 by author(s).
Applied Chemical Engineering is published by Arts and Science Press Pte. Ltd. This work is licensed under the Creative Commons Attribution-NonCommercial 4.0 International License (CC BY 4.0).
https://creativecommons.org/licenses/by/4.0/

1. Introduction

Amino acids have a particularly important location in biology as basic building blocks of all proteins and contribute to cellular functions[1,2]. The terms dissociation/protonation constants are used to measure of acidic or alkaline force. The term ionization constant is used in the case of zwitterions[3,4]. In a strong basic medium, amino acids can behave as acids, losing their protons and becoming anions. In a strong basic medium, however, they can behave as bases, gaining a proton and becoming positive ions (cations). Ionization constants (pKa) are fundamental values that express the strength of an acid or base and the tendency of a molecule to dissociate in solution. These values can be determined in several ways, including experimental methods such as potentiometric titration, which relies on measuring the change in electrical potential when a base or acid is added. Spectroscopic methods such as ultraviolet–visible (UV–Vis) or nuclear magnetic resonance (NMR) are used to track changes in absorption or chemical displacement[5-7]. Theoretical computational methods such as density functional theory (DFT) can also be used to calculate pKa values for the neutral and negative states of a molecule. These theoretical methods provide high accuracy in predicting ionization values, especially when practical measurements are difficult, and are currently widely used in chemistry and drug design to understand the

behavior of molecules in different media. This theory is based on the principle that the properties of an atomic or molecular system can be determined by the distribution of electron density rather than complex wave functions[8-10]. Basis sets are a set of mathematical functions used to represent atomic and electron orbitals in theoretical calculations. The most common bases are 6-311G(d,p) and cc-pVDZ, which differ in computational precision and the number of functions used to describe the electrons. Choosing the appropriate base is crucial to achieving a balance between the accuracy of the results and the computational effort required[11,12]. DFT is widely used to calculate energies, lengths, angles, ionization constants, and chemical reactions with acceptable accuracy and low computational cost compared to other quantitative methods[13-16]. Energy variables such as HOMO and LUMO are among the most important indicators for understanding the behavior of molecules in chemical reactions. HOMO represents a molecule's ability to donate electrons, while LUMO expresses its ability to gain them[17,18]. The difference between them (the energy gap) is an indicator of a molecule's activity and stability, as a small energy gap indicates ease of ionization and a low pKa value. Hardness reflects a molecule's resistance to changes in its electron configuration; the higher the hardness[19-20], the lower its ionization potential. Chemical potential and electrophilicity determine a molecule's tendency to lose or gain electrons, which helps estimate its acidic or basic strength. Mulliken charge analysis reveals the charge distribution within a molecule, helping to identify the active sites involved in the ionization process[21,22]. The importance of these variables in theoretical calculations lies in the fact that they enable researchers to accurately estimate the values of ionization constants and compare them with experimental values, which helps in gaining a deeper understanding of the behavior of compounds and explaining the differences in results between experiments and theoretical models.

2. Experimental and computational methods

A series of amino acid derivatives was synthesized by reacting selected amino acids—glycine, serine, threonine, valine, and leucine—with the active reagent 2,4-dinitrophenyl, a classical method for amino acid derivatization[18]. The synthesized compounds were characterized using Fourier transform infrared (FTIR) spectroscopy to confirm their predicted molecular structure. The spectra showed characteristic absorption bands for the nitro group (NO_2) in the 1350–1530 cm^{-1} range and strong expansion bands for the carbonyl group (C=O) in the 1650–1680 cm^{-1} range, confirming the structural integrity of the synthesized derivatives.

The 2,4-DNP-Serine compound exhibits broad optical wavelengths at 3300–3400 cm^{-1}, corresponding to the hydroxyl (OH) group in the curtain. A less pronounced boundary was observed in the 2,4-DNP-Threonine compound, attributed to the directional discovery of its functional properties[23-26].

Figures 1 and **2** show the FTIR spectra of 2,4-DNP-Serine and 2,4-DNP-Threonine, respectively, showing the clear agreement between the spectral data and the proposed molecular structures.

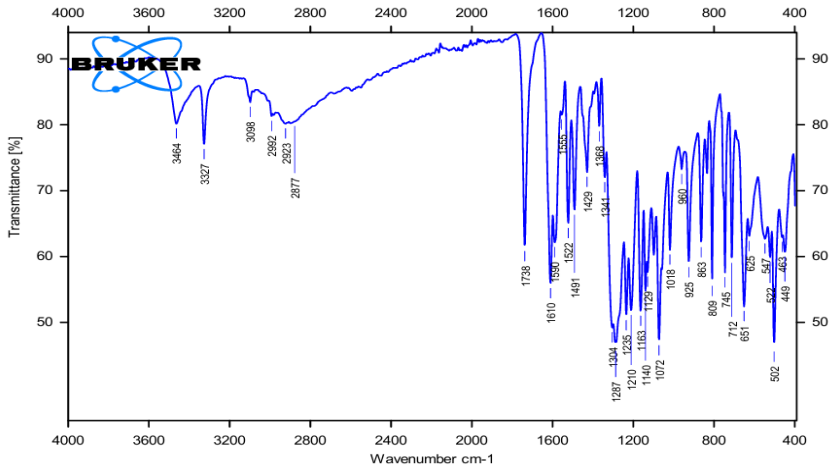

Figure 1. FTIR Spectrum of the prepared 2,4-Dinitrophenyl-Serene compound.

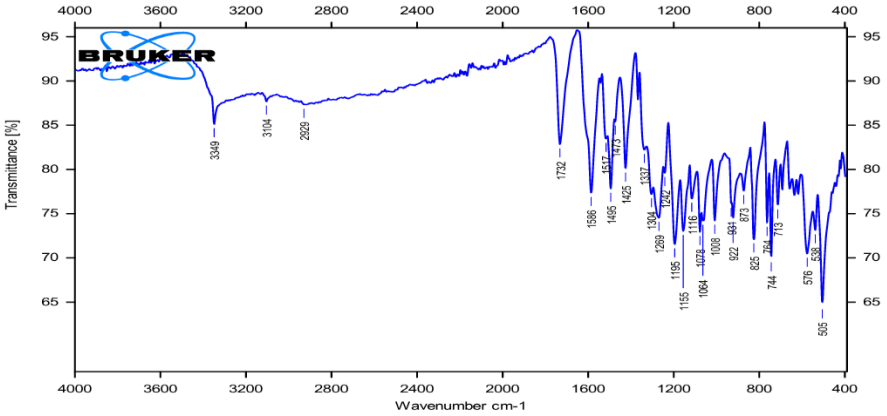

Figure 2. FTIR Spectrum of the prepared 2,4-Dinitrophenyl-threonine compound.

The ionization constants (pKa values) of these derivatives were then determined experimentally by pH-metric titration. A calibrated pH meter was used to monitor the pH of aqueous solutions during incremental addition of a standardized base. The resulting titration curves (pH versus titrant volume) were analyzed to identify the half-neutralization points, at which the measured pH equals the experimental pKa of the compound[27].

For the theoretical study, molecular structures were optimized using Density Functional Theory (B3LYP) with the 6-311G(d,p) and cc-pVDZ basis sets, following recent benchmarks that demonstrated their reliability in modeling amino acid ionization equilibria The B3LYP function and the two base sets 6-311G(d,p) and cc-pVDZ were chosen due to their proven accuracy in calculating pKa and ionization balances of amino acids. B3LYP combines accuracy and efficiency, while 6-311G(d,p) provides a more detailed representation of the polarized electrons on oxygen and nitrogen atoms, and cc-pVDZ is a computationally efficient option with acceptable accuracy. Reference studies have confirmed the reliability of this combination in predicting pKa values with high accuracy[28,29].

From the optimized geometries, a set of quantum-chemical descriptors was extracted, including frontier orbital energies (EHOMO, ELUMO), the HOMO–LUMO gap, Mulliken atomic charges, dipole moments, and selected bond lengths related to ionizable groups. These descriptors were calculated for both the neutral (zwitterionic) and anionic states of each derivative[30,31].

Instead of applying the direct thermodynamic relation between ΔG and pKa, a quantitative structure–property relationship (QSPR) approach was employed. The experimentally determined pKa values were correlated with the theoretical descriptors using linear regression, consistent with modern cheminformatics applications[32] Variables showing the highest correlation coefficients were selected, and regression models were constructed to predict pKa. The models were statistically validated by calculating the correlation coefficient (R^2), adjusted R^2, and the root-mean-square error (RMSE), which provided direct measures of predictive accuracy and reliability[33].

3. Results and discussion

The correlation analysis between DFT-derived quantum-chemical descriptors and experimental pKa values was carried out for both the neutral and the anionic states. Mulliken atomic charges, frontier orbital energies, the HOMO–LUMO gap, dipole moments, and selected bond lengths were evaluated using B3LYP with the 6-311G(d,p) and cc-pVDZ basis sets[34]. For the neutral state, **Tables 1** and **2** summarize the Mulliken charges calculated for atoms C1, C2, C3, N4, C5, H6, C7, O8, and O9.

The results indicate that the charges on O8, N4, exhibit the highest correlation with experimental pKa values (R > 0.9(because they constitute the main ionizable sites in the molecule. O8 represents the oxygen

atom in the carboxyl group responsible for proton loss, while N4 represents the amino nitrogen atom that contributes to the stability of the conjugated base through hydrogen bonding and resonance effects. Therefore, the change in charge distribution around these two atoms largely controls the ease of ionization and the pKa value.

This demonstrates that electron density distribution around the ionizable functional groups is a key determinant of acidity in the neutral state. Consistent with recent computational findings on charge localization and acidity scales[35].

Table 1. Theoretical physical variables of neutral compounds calculated by then DFT/6-311G (d,p) method.

compounds	Charge on an atom								S.E	Dipol-Dipol	VDW
	C_1	C_2	C_3	N_4	C_5	H_6	C_7	O_8			
2,4-Di-nitrophenyl-glycine	0.1158	0.2941	-0.1498	-0.4837	-0.0744	0.1647	0.3214	-0.3183	1.1849	8.0129	10.2370
2,4-Di-nitrophenyl-alanine	0.1122	0.2903	-0.1402	-0.4557	-0.1010	0.1615	0.3679	-0.3199	1.3130	7.9935	10.8984
2,4-Di-nitrophenyl-serine	0.1117	0.2869	-0.1310	-0.4632	-0.1086	0.1621	0.3768	-0.3276	1.4173	8.1675	11.3748
2,4-Di-nitrophenyl-Threonine	0.1111	0.2401	-0.1176	-0.4589	-0.0788	0.1659	0.3729	-0.3239	1.5494	9.4461	12.0072
2,4-Di-nitrophenyl-valine	0.1096	0.2822	-0.1373	-0.4465	-0.0424	0.1645	0.3730	-0.3159	2.7592	5.9424	13.9831
2,4-Di-nitrophenyl-leucine	0.1121	0.2824	-0.1347	-0.7523	-0.0903	0.1656	0.3803	-0.3232	3.4457	6.00	14.9844

Table 2. Theoretical physical variables of neutral compounds calculated by the DFT/cc-pVDZ method.

compounds	Charge on an atom								S.E	Dipol-Dipol	VDW
	C_1	C_2	C_3	N_4	C_5	H_6	C_7	O_8			
2,4-Di-nitrophenyl-glycine	0.1390	0.0768	0.0091	-0.1485	0.1143	0.0704	0.1409	-0.1553	1.1849	8.0129	10.2370
2,4-Di-nitrophenyl-alanine	0.1378	0.0667	0.0203	-0.1078	-0.0214	0.0426	0.1900	-0.1570	1.3130	7.9935	10.8984
2,4-Di-nitrophenyl-serine	0.1397	0.0578	0.0265	-0.1225	0.0136	0.0404	0.1921	-0.1673	1.4173	8.1675	11.3748
2,4-Di-nitrophenyl-Threonine	0.1387	0.0165	0.0385	-0.1204	0.0529	0.0324	0.1895	-0.1574	1.5494	9.4461	12.0072
2,4-Di-nitrophenyl-valine	0.1365	0.0516	0.0275	-0.1072	0.0834	0.0198	0.1780	-0.1578	2.7592	5.9424	13.9831
2,4-Di-nitrophenyl-leucine	0.1383	0.0489	0.0306	-0.1094	0.0274	0.0192	0.1976	-0.1617	3.4457	6.00	14.9844

For the anionic state, **Table 3** provides the Mulliken charges obtained after deprotonation. Here, the correlation analysis reveals that changes in the charges on O8 and N4 remain dominant predictors of ionization constants, although the overall R values are slightly lower than those observed in the neutral state. This reduction reflects the increased sensitivity of the anionic species to solvation and conformational effects, as also reported in recent amino acid modeling studies[36].

Table 3. Theoretical physical variables of anionic compounds calculated by the DFT/6-311G method.

Compounds	Charge on an atom								S.E	Dipole-Dipole	VDW
	C_1	C_2	C_3	N_4	C_5	H_6	C_7	O_8			
2,4-Di-nitrophenyl-glycine	.0283	.4386	-.2068	-.5718	-.0834	.1007	.5030	-.6197	2.5660	6.6754	11.0359
2,4-Di-nitrophenyl-alanine	.1117	.2891	-.1400	-.3986	-.1606	.1140	.3328	-.4790	2.7411	6.5061	11.7733
2,4-Di-nitrophenyl-serine	.1135	.2910	-.0872	-.3991	-.1898	.1176	.3811	-.4921	2.6810	6.1554	13.2082
2,4-Di-nitrophenyl-Threonine	.1124	.2850	-.1404	-.4033	-.1473	.1254	.3468	-.4750	2.7539	6.0839	14.2774
2,4-Di-nitrophenyl-valine	.1070	.2762	-.1252	-.3945	-.1080	.1073	.3498	-.4741	3.0411	6.5464	13.1773
2,4-Di-nitrophenyl-leucine	.1207	.2561	-.0997	-.4459	-.1122	.1183	.3593	-.4597	3.0856	6.4028	13.9444

The results collectively highlight that, under DFT calculations, the Mulliken charges—especially on O8 and N4—along with the HOMO–LUMO energy gap, serve as the most reliable descriptors for predicting pKa in both neutral and anionic states.

The graphical representations clarified the central role of electronic structure in determining ionization behavior. O8 represents the most electronegative atom, where the negative charge was more pronounced and stronger with (6-311G)(d,p) is (−0.16).

This suggests that (6-311G)(d,p) favors charge localization at electronegative sites, while (cc-pVDZ) distributes the charge more broadly across the molecule. As depicted in the **Figure 3**.

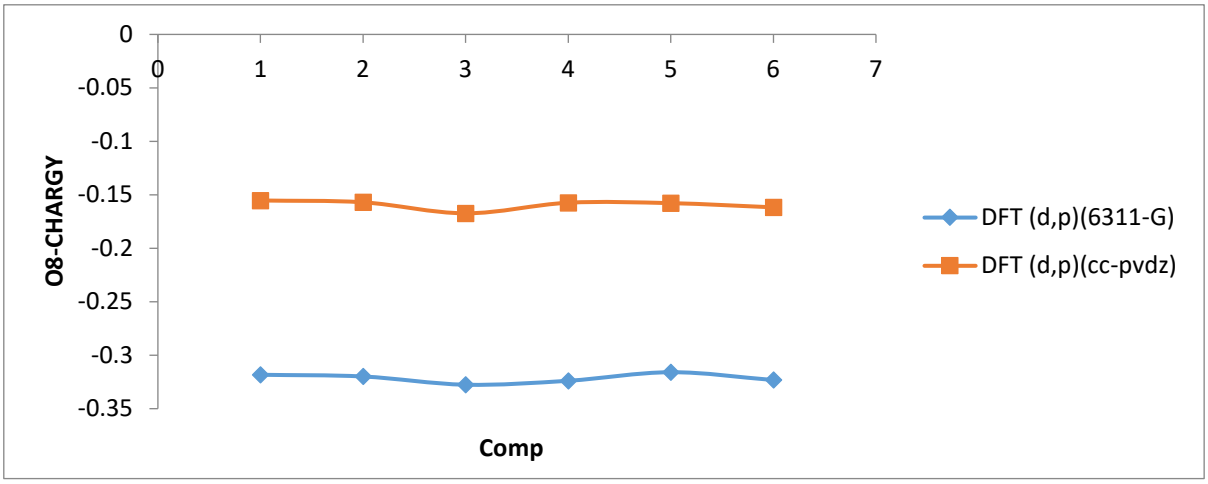

Figure 3. Relationship between the neutral Mulliken charges of the oxygen atom calculated using DFT with two basis sets: (cc-pVDZ) and(6-311G)(d,p).

The experimental and theoretical pKa values of the studied amino acid derivatives were analyzed under both the neutral and anionic states, with calculations carried out using the DFT/B3LYP method and two different basis sets: 6-311G (d,p) and cc-pVDZ.

The aim was to evaluate the predictive accuracy of these basis sets relative to the experimentally measured ionization constants obtained from pH-metric titration. Comparative Evaluation of Experimental and DFT/6-311G(d,p), Predicted pKa Values for Neutral and Anionic Amino Acid Derivatives.

A first set of calculations refers to a comparison between the experimental pKa values and those calculated with the 6-311G(d,p) basis set for the neutral (zwitterionic) form.

Table 4. Experimental and theoretical pKa values for neutral amino acid derivatives DFT 6311-G (d,p).

Compound	DFT 6311-G (d,p)		
	pKa*	pKa**	ΔpKa
2,4-Di-nitrophenyl-glycine	3.589	3.581	0.0080
2,4-Di-nitrophenyl-alanine	1.934	2.045	-0.1110
2,4-Di-nitrophenyl-serine	3.151	2.951	0.2000
2,4-Di-nitrophenyl-Threonine	3.439	3.527	-0.0880
2,4-Di-nitrophenyl-valine	3.563	3.525	0.0380
2,4-Di-nitrophenyl-leucine	3.642	3.392	0.2500

From **Table 4**, it is evident that the deviations between experimental and theoretical pKa values are relatively small, generally within the range of −0.11 to +0.25 units. This indicates that the inclusion of polarization functions (d,p) in the 6-311G(d,p) basis set enhances the description of electron density around the ionizable groups, thereby improving the prediction of ionization constants in the neutral state. Overall, the agreement with experiment demonstrates the reliability of this basis set for modeling zwitterionic amino acid derivatives.

A second set of calculations was performed for the neutral state using the cc-pVDZ basis set, and the results are summarized in **Table 5**.

Table 5. Experimental and theoretical pKa values for neutral amino acid derivatives DFT (cc-pVDZ).

Compound	DFT- cc-pVDZ		
	pKa*	pKa**	ΔpKa
2,4-Di-nitrophenyl-glycine	3.589	3.5678	0.0212
2,4-Di-nitrophenyl-alanine	1.934	1.9246	0.0094
2,4-Di-nitrophenyl-serine	3.151	3.2404	-0.0894
2,4-Di-nitrophenyl-Threonine	3.439	3.3959	0.0431
2,4-Di-nitrophenyl-valine	3.563	3.5121	0.0509
2,4-Di-nitrophenyl-leucine	3.642	3.6769	-0.0349

The cc-pVDZ results also show acceptable agreement with experiment, but the deviations tend to be slightly larger for some derivatives, particularly those with nonpolar side chains. This suggests that while cc-pVDZ provides a computationally less expensive option, it does not always capture subtle polarization and hydrogen-bonding effects with the same level of accuracy as 6-311G(d,p). When comparing both basis sets in the neutral state, 6-311G(d,p) consistently yields smaller deviations and therefore appears to be the more accurate choice.

This aligns with the consensus that polarization functions and extended basis sets enhance predictive performance in proton transfer simulations[37].

Third set performance of the 6-311G (d,p) basis set was further evaluated in the anionic state, where deprotonation occurs. The comparison of experimental and theoretical values is provided in **Table 6**.

Table 6. Experimental and theoretical pKa values for anionic amino acid derivatives DFT 6311-G (d,p).

Compound	DFT 6311-G (d,p)		
	pKa*	pKa**	ΔpKa
2,4-Di-nitrophenyl-glycine	3.589	3.5811	0.0079
2,4-Di-nitrophenyl-alanine	1.934	1.9482	-0.0142
2,4-Di-nitrophenyl-serine	3.563	3.5282	0.0348
2,4-Di-nitrophenyl-Threonine	3.439	3.3977	0.0413
2,4-Di-nitrophenyl-valine	3.151	3.1588	-0.0078
2,4-Di-nitrophenyl-leucine	3.642	3.6524	-0.0104

The calculated pKa values for the anionic forms are generally in good agreement with the experimental data, with most deviations remaining within ±0.3 units. The discrepancies observed for certain derivatives may be attributed to the increased sensitivity of the anionic state to solvation and hydrogen-bonding effects, which are not fully captured in implicit solvation models. Nevertheless, the overall performance of 6-311G(d,p) in the anionic state demonstrates that it can reliably reproduce experimental ionization constants with reasonable accuracy. Overall Comparison the results clearly indicate that the choice of basis set plays a decisive role in the predictive accuracy of theoretical pKa calculations. For the neutral state, 6-311G(d,p) provided the closest match to experimental values, because this structure represents the predominant form of amino acids in aqueous medium at neutral pH (pH ≈ 7). In this case, the electrostatic attraction forces within the molecule are more stable, which reduces the effect of the solvent and surrounding reactive factors and makes the electron density distribution closer to experimental reality, while cc-pVDZ delivered acceptable but slightly less accurate results. For the anionic state, the 6-311G(d,p) basis set again showed reliable performance with small deviations from experiment. In summary, 6-311G(d,p) represents the more accurate and balanced basis set for predicting ionization constants of amino acid derivatives, performing well across both neutral and anionic states. The cc-pVDZ basis set remains a useful alternative in neutral systems when computational efficiency is a priority, though with a trade-off in predictive accuracy.

4. Conclusion

The study confirmed that the DFT/B3LYP method provides accurate predictions of amino acid derivatives' pKa values, showing strong agreement with experimental data. Among the examined basis sets, 6-311G(d,p) achieved the highest precision, while cc-pVDZ delivered reasonable accuracy with lower computational cost. Mulliken charges on oxygen and nitrogen atoms, and the HOMO–LUMO gap were identified as major determinants of acidity. The neutral (zwitterionic) forms correlated better with experimental values than the anionic species. Deviations between theoretical and experimental results remained within ±0.3 pKa units, confirming strong predictive validity. The integration of theoretical and experimental findings improved the understanding of proton transfer mechanisms. Overall, these results highlight the usefulness of DFT-based approaches in biochemical and drug design applications.

Conflict of interest

The authors declare no conflict of interest.

Refernces

1. Nelson, D. L., & Cox, M. M. (2017). Lehninger Principles of Biochemistry (7th ed.). W. H. Freeman.
2. Voet, D., & Voet, J. G. (2011). Biochemistry (4th ed.). John Wiley & Sons.
3. Alcázar, J. J., Misad Saide, A. C., & Campodónico, P. R. (2023). Reliable and accurate prediction of basic pKa values in nitrogen compounds. Journal of Cheminformatics, 15(1), 90. https://doi.org/10.1186/s13321-023-00763-3
4. Warshel, A., Sharma, P. K., Kato, M., Xiang, Y., Liu, H., & Olsson, M. H. (2006). Electrostatic basis for enzyme catalysis. Chemical Reviews, 106(8), 3210–3235. https://doi.org/10.1021/cr0503106
5. Kamerlin, S. C., & Warshel, A. (2010). At the dawn of the 21st century: Is dynamics the missing link for understanding enzyme catalysis? Proteins, 78(6), 1339–1375. https://doi.org/10.1002/prot.22654
6. Zuchniarz, J., et al. (2022). Accurate pKa calculations in proteins with reactive molecular dynamics provide physical insight. Journal of Chemical Theory and Computation, 18(12), 7451–7464. https://doi.org/10.1021/acs.jctc.2c00864
7. Khan, M. S., et al. (2019). Potentiometric titrations for accurate determination of ionization constants of biomolecules. Journal of Chemical Education, 96(6), 1182–1187. https://doi.org/10.1021/acs.jchemed.9b00045
8. Granot, J. (1983). Determination of equilibrium constants by NMR spectroscopy. Progress in NMR Spectroscopy, 15(2), 105–156. https://doi.org/10.1016/0079-6565(83)80001-5
9. Alegaon, S. G., et al. (2022). Experimental evaluation of pKa values of amino acid analogues in aqueous media. Journal of Molecular Liquids, 360, 119430. https://doi.org/10.1016/j.molliq.2022.119430
10. Butler, J. N. (1998). Ionic Equilibrium: Solubility and pH Calculations. Wiley.
11. Cramer, C. J. (2013). Essentials of Computational Chemistry: Theories and Models (2nd ed.). Wiley.
12. Parr, R. G., & Yang, W. (1994). Density-Functional Theory of Atoms and Molecules. Oxford University Press.
13. Koch, W., & Holthausen, M. C. (2015). A Chemist's Guide to Density Functional Theory (2nd ed.). Wiley-VCH.
14. Othman, A. Y. , Saleh, M. Y. and Owaid, K. A. (2025). Recyclable Bio-Functionalized Graphene Oxide Nanocatalyst for Sustainable and High-Yield Synthesis of Arylimine-Substituted Benzo[b]pyridonaphthyridin-7-one Derivatives in Water. Journal of Nanostructures, 15(3), 1463-1474. doi: 10.22052/JNS.2025.03.060
15. Dutra, F. R., de Souza Silva, C., & Custódio, R. (2021). On the accuracy of the direct method to calculate pKa from electronic structure calculations. Journal of Physical Chemistry A, 125(1), 65–73. https://doi.org/10.1021/acs.jpca.0c09743
16. Saeed, N. H., et al. (2025). Computational study on the Estramustine (EMCYT) and its active metabolites anticancer drugs 17-α-estradiol and nornitrogen. Results in Chemistry, 102747. https://doi.org/10.1016/j.rechem.2025.102747
17. Muna S. Aldulaimi, Shakir M. Saied, Salim J. Mohammed, & Mohanad Y. Saleh. (2025). Using green chemistry (deep eutectic solvents) to synthesize pyrazol-4-yl-thiazolidin-4-one derivatives and evaluate their antibacterial activity. Applied Chemical Engineering, 8(3), ACE-5708. https://doi.org/10.59429/ace.v8i3.5708
18. Abed, A. N., & A Ibrahim, A. (2021). Theoretical, Voltammetric and Thermodynamic study for Cadmium (II)-Tyrosine Complex at 293-313 K. Egyptian Journal of Chemistry, 64(10), 5555-5559.
19. Ali, A. H., Saleh, M. Y., & Owaid, K. A. (2023). Mild Synthesis, Characterization, and Application of some Polythioester Polymers Catalyzed by Cetrimide Ionic Liquid as a Green and Eco-Friendly Phase-Transfer Catalyst. Iranian Journal of Catalysis, 13(1).
20. Li, X., Gao, Y., & Pan, D. (2023). Recent advances in computational prediction of pKa values and their applications in drug discovery. Expert Opinion on Drug Discovery, 18(7), 639–653. https://doi.org/10.1080/17460441.2023.2208765
21. Alshdoukhi, I. F., et al. (2024). Pd (II), Pt (II), Zn (II), Cd (II) and Hg (II) complexes of the newly prepared 1, 2-benzo-isothiazol-3 (2H)-dithiocarbamate (BIT-DTC) ligand. Bulletin of the Chemical Society of Ethiopia, 38(4), 889-899. DOI: https://dx.doi.org/10.4314/bcse.v38i4.6
22. Ibrahim, A. A., & Yahya, R. (2012). Electrochemical study of the complexation of methyl yellow with some metal ions as a model for doped polyazo compound. Asian Journal of Chemistry, 24(6), 2634.
23. Rao, K. R., & Sober, H. A. (1954). Preparation and properties of 2,4-dinitrophenyl-L-amino acids. Journal of the American Chemical Society, 76(5), 1328–1331. https://doi.org/10.1021/ja01634a041
24. Al-Thakafy, N. T., Abdelzaher, M. A., Abdelzaher, H. G., Saleh, M. Y., Al-Enizzi, M. S., Saied, S. M., ... & Moghanm, F. S. (2024). A novel chalcone compound as a reagent for the validation of pharmaceutical cefotaxime sodium preparations. Results in Chemistry, 7, 101387.
25. Hamdoon, A. M., Al-Iraqi, M. A., & Saleh, M. Y. (2022). Synthesis of some multi-cyclic sulfhydryl donor compounds containing 1, 2-dithiol-3-thione moiety. Egyptian Journal of Chemistry, 65(3), 427-434.
26. Saleh, M. Y., Al-barwari, A. S., & Ayoob, A. I. (2022). Synthesis of some novel 1, 8-naphthyridine chalcones as antibacterial agents. Journal of Nanostructures, 12(3), 598-606.

27. Alhazmi, H. A. (2019). Fourier transform infrared (FTIR) spectroscopy for amino acid and protein structure analysis. Applied Spectroscopy Reviews, 54(8), 682–699. https://doi.org/10.1080/05704928.2018.1535423
28. Wappett, D. A., & Goerigk, L. (2023). Benchmarking density functional theory methods for metalloenzyme reactions: The introduction of the mme55 set. Journal of Chemical Theory and Computation, 19(22), 8365-8383.
29. Sebesta, F., Sovova, Z., & Burda, J. V. (2024). Determination of amino acids'p K a: importance of cavity scaling within implicit solvation models and choice of DFT functionals. The Journal of Physical Chemistry B, 128(7), 1627-1637.
30. Saleh, M. Y., Aldulaimi, A. K. O., Saeed, S. M., & Adhab, A. H. (2025). Palladium fabricated on Fe3O4 as an organic-inorganic hybrid nanocatalyst for the Suzuki and Stille coupling reactions. Journal of Molecular Structure, 1321, 139597.
31. Sheet, S. H., et al. (2024). Theoretical study for comparison of pka of a number of schiff bases by employing parameters derived from dft and mp2 method. New Materials, Compounds and Applications, 8(1), 94-108. https://doi.org/10.62476/nmca8194
32. Hasb, A. M., & Saeed, N. H. (2025). CHLORINATION OF N-BENZOYL VALINE BY SODIUM N-CHLORO-PARA-TOLUENE SULFONYL AMIDE (CAT) HYDROCHLORIC ACIDIC: A KINETIC AND MECHANISM STUDY. Kimya Problemleri, 23(2), 239-248. DOI: 10.32737/2221-8688-2025-2-239-248
33. Mohammedthalji, N. H., et al (2022). Thermodynamic & Kinetic Study of the Adsorption of Glycolic acid using a Natural Adsorbent. Egyptian Journal of Chemistry, 65(6), 505-520. 10.21608/ejchem.2022.119362.5365
34. Zeng, Q., et al. (2018). Absolute and relative pKa predictions via a DFT approach: SAMPL6 challenge. Journal of Computer-Aided Molecular Design, 32(10), 1071–1085. https://doi.org/10.1007/s10822-018-0158-5
35. Šebesta, F., et al. (2024). Determination of amino acids' pKa: Importance of cavity scaling within implicit solvation models. Journal of Physical Chemistry B, 128(7), 1903–1912. https://doi.org/10.1021/acs.jpcb.3c09021
36. Fazeli, A., et al. (2023). Predicting pKa of the carboxylic acid group in water for amino acids. Computational and Theoretical Chemistry, 1235, 113984. https://doi.org/10.1016/j.comptc.2023.113984
37. Mayr, F., Wieder, M., & Wieder, O. (2022). Improving small molecule pKa prediction using transfer learning with graph neural networks. Frontiers in Chemistry, 10, 866585. https://doi.org/10.3389/fchem.2022.866585